Topology of the $O(3)$ non-linear sigma model under the gradient flow

Stuart Thomas

Christopher Monahan

May 3, 2021

Topology of the $O(3)$ non-linear sigma model under the gradient flow

Stuart Thomas

Christopher Monahan

May 3, 2021

particles $\Rightarrow$ fields

[1] B. Odom et al., Phys. Rev. Lett. **97**, 030801 (2006).

particles $\Rightarrow$ fields

- particle physics and condensed matter

[1] B. Odom et al., Phys. Rev. Lett. **97**, 030801 (2006).

particles $\Rightarrow$ fields

- particle physics and condensed matter
- incorporates many-particle quantum mechanics and special relativity

[1] B. Odom et al., Phys. Rev. Lett. **97**, 030801 (2006).

particles $\Rightarrow$ fields

- particle physics and condensed matter
- incorporates many-particle quantum mechanics and special relativity
- remarkably accurate[1]

[1] B. Odom et al., Phys. Rev. Lett. **97**, 030801 (2006).

Path Integral Formulation

"quantum principle of least action"

$$\langle \hat{O} \rangle = \frac{1}{Z} \int \mathcal{D}\phi \, \hat{O}[\phi] \, e^{iS[\phi]}$$

Wick Rotation

$$t \Rightarrow it$$

Minkowski Spacetime $\Rightarrow$ Euclidean Spacetime

Wick Rotation

$$t \Rightarrow it$$

Minkowski Spacetime $\Rightarrow$ Euclidean Spacetime

$$\langle \hat{O} \rangle = \frac{1}{Z} \int \mathcal{D}\phi \, \hat{O}[\phi] \, e^{iS[\phi]}$$

$$\Downarrow$$

$$\langle \hat{O} \rangle = \frac{1}{Z} \int \mathcal{D}\phi \, \hat{O}[\phi] \, e^{-S_E[\phi]}$$

Wick Rotation

$$t \Rightarrow it$$

$$\text{Minkowski Spacetime} \Rightarrow \text{Euclidean Spacetime}$$

$$\langle \hat{O} \rangle = \frac{1}{Z} \int \mathcal{D}\phi \, \hat{O}[\phi] \; e^{iS[\phi]}$$

$$\Downarrow$$

$$\langle \hat{O} \rangle = \frac{1}{Z} \int \mathcal{D}\phi \, \hat{O}[\phi] \; e^{-S_E[\phi]}$$

ϕ^4 model

Euclidean Action

$$S_E[\phi] = \int d^2x_E \left[\frac{1}{2}\left(\partial_t\phi\right)^2 + \frac{1}{2}\left(\partial_x\phi\right)^2 + \frac{1}{2}m_0^2\phi^2 + \frac{\lambda}{4}\phi^4\right]$$

- real scalar field
- describes a boson
- spontaneous symmetry breaking at $\lambda = 0.5$, $m_0^2 = -0.72$

Non-Linear σ Model

Euclidean Action

$$S_E = \frac{\beta}{2} \int d^2x \; \left[(\partial_t \vec{e})^2 + (\partial_x \vec{e})^2 \right]$$

- $O(3)$ non-linear sigma model (NLSM) in 1+1 dimensions

Non-Linear σ Model

Euclidean Action

$$S_E = \frac{\beta}{2} \int d^2x \ \left[(\partial_t \vec{e})^2 + (\partial_x \vec{e})^2 \right]$$

- $O(3)$ non-linear sigma model (NLSM) in 1+1 dimensions
- $\vec{e}$ is 3-component vector constrained by $|\vec{e}| = 1$

Non-Linear σ Model

Euclidean Action

$$S_E = \frac{\beta}{2} \int d^2x \; \left[(\partial_t \vec{e})^2 + (\partial_x \vec{e})^2 \right]$$

- $O(3)$ non-linear sigma model (NLSM) in 1+1 dimensions
- $\vec{e}$ is 3-component vector constrained by $|\vec{e}| = 1$
- Applications
  - Prototypical model for strong nuclear force
  - Models Heisenberg ferromagnets
  - Applications to string theory

Non-Linear σ Model

Euclidean Action

$$S_E = \frac{\beta}{2} \int d^2x \; \left[(\partial_t \vec{e})^2 + (\partial_x \vec{e})^2 \right]$$

- $O(3)$ non-linear sigma model (NLSM) in 1+1 dimensions
- $\vec{e}$ is 3-component vector constrained by $|\vec{e}| = 1$
- Applications
  - Prototypical model for strong nuclear force
  - Models Heisenberg ferromagnets
  - Applications to string theory
- Merits
  - mass gap
  - asymptotic freedom

Topology of 1+1 $O(3)$ NLSM

1. Envision spacetime as a sphere

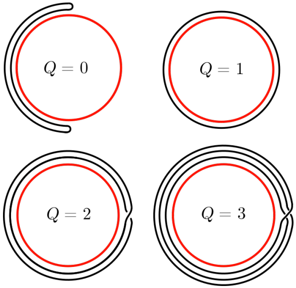

Figure: Homotopy group of $S^1 \to S^1$

[2] P. Goddard and P. Mansfield, Rep. Prog. Phys. **49**, 725 (1986)
[3] A. Y. Kitaev, Russ. Math. Surv. **52**, 1191 (1997)

Topology of 1+1 $O(3)$ NLSM

1. Envision spacetime as a sphere
2. The NLSM field $\vec{e}$ becomes mapping between Riemann spheres ($S^2 \to S^2$).

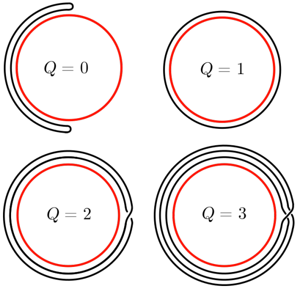

Figure: Homotopy group of $S^1 \to S^1$

[2] P. Goddard and P. Mansfield, Rep. Prog. Phys. **49**, 725 (1986)
[3] A. Y. Kitaev, Russ. Math. Surv. **52**, 1191 (1997)

Topology of 1+1 $O(3)$ NLSM

1. Envision spacetime as a sphere
2. The NLSM field $\vec{e}$ becomes mapping between Riemann spheres ($S^2 \to S^2$).
3. Associates every configuration with topological charge Q

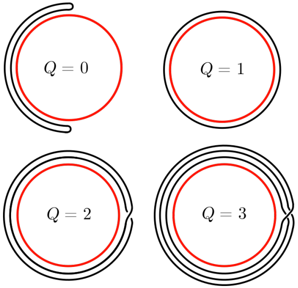

Figure: Homotopy group of $S^1 \to S^1$

[2] P. Goddard and P. Mansfield, Rep. Prog. Phys. **49**, 725 (1986)
[3] A. Y. Kitaev, Russ. Math. Surv. **52**, 1191 (1997)

Topology of 1+1 $O(3)$ NLSM

1. Envision spacetime as a sphere
2. The NLSM field $\vec{e}$ becomes mapping between Riemann spheres ($S^2 \to S^2$).
3. Associates every configuration with topological charge Q
4. Topology is important to cosmology[2] and fault-tolerant quantum computing[3].

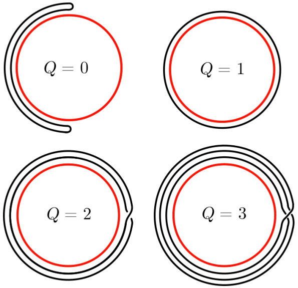

Figure: Homotopy group of $S^1 \to S^1$

[2] P. Goddard and P. Mansfield, Rep. Prog. Phys. **49**, 725 (1986)
[3] A. Y. Kitaev, Russ. Math. Surv. **52**, 1191 (1997)

Non-trivial NLSM

$$S[\vec{e}] \to S[\vec{e}] - i\theta Q[\vec{e}].$$

Nonzero θ implies nonzero $\langle Q \rangle$.

Topological Susceptibility

Proportional to variance of topological charge

$$\chi_t \equiv \frac{\langle Q^2 \rangle - \langle Q \rangle^2}{L^2}$$

Topological Susceptibility

Proportional to variance of topological charge

$$\chi_t \equiv \frac{\langle Q^2 \rangle - \langle Q \rangle^2}{L^2}$$

In trivial NLSM:

$$\chi_t = \frac{\langle Q^2 \rangle}{L^2}$$

In nontrivial NLSM:

$$\chi_t \propto \frac{\partial \langle Q \rangle}{\partial \theta}$$

Topological Susceptibility

Proportional to variance of topological charge

$$\chi_t \equiv \frac{\langle Q^2 \rangle - \langle Q \rangle^2}{L^2}$$

In trivial NLSM:

$$\chi_t = \frac{\langle Q^2 \rangle}{L^2}$$

In nontrivial NLSM:

$$\chi_t \propto \frac{\partial \langle Q \rangle}{\partial \theta}$$

Main Problem

Topological stability predicts $\chi_t = 0$, but χ_t diverges in numerical results[a].

[a] B. Berg and M. Lüscher, Nuclear Physics B **190**, 412 (1981).

The Gradient Flow

- Successful in removing χ_t divergence in QCD (model of the strong nuclear force).

The Gradient Flow

- Successful in removing χ_t divergence in QCD (model of the strong nuclear force).
- Reduces high-momentum modes

The Gradient Flow

- Successful in removing χ_t divergence in QCD (model of the strong nuclear force).
- Reduces high-momentum modes
- Introduces a new dimension, τ, called the "flow time," which pushes fields towards action minima

The Gradient Flow

- Successful in removing χ_t divergence in QCD (model of the strong nuclear force).
- Reduces high-momentum modes
- Introduces a new dimension, τ, called the "flow time," which pushes fields towards action minima
- In the ϕ^4 model

$$\frac{\partial \rho(\tau, x)}{\partial \tau} = \partial^2 \rho(\tau, x)$$

with the boundary condition $\rho(0, x) = \phi(x)$.

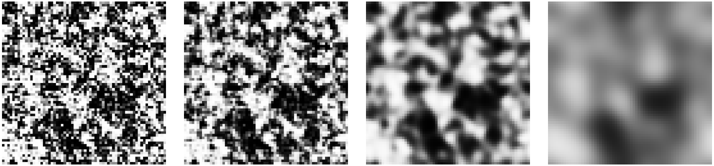

(a) $\tau = 0$ **(b)** $\tau = 0.001$ **(c)** $\tau = 0.01$ **(d)** $\tau = 0.1$

Figure: Effect of flow time evolution on a random lattice in the symmetric phase. White represents positive values of ϕ while black represents negative.

Research Question

Can the gradient flow remove the topological susceptibility divergence in the NLSM?

Methods

1. Construct Monte Carlo simulation following Euclidean path integral formalism
2. Apply gradient flow to configurations
3. Measure topological susceptibility

Fields on the Lattice

$$x \to ia\hat{t} + ja\hat{x}$$

$$\int dtdx \to a^2 \sum_i$$

where a is the lattice spacing.

Periodic boundary conditions:

$$\phi\left(x_{i+L,j}\right) = \phi\left(x_{i,j+L}\right) = \phi\left(x_{i,j}\right)$$

Markov chain Monte Carlo

Due to Boltzmann factor e^{-S}, we need only consider configurations near action minima.

Markov chain Monte Carlo

Due to Boltzmann factor e^{-S}, we need only consider configurations near action minima.

- Starting at configuration ϕ_a, we transition to configuration ϕ_b with probability

$$P(\phi_a \to \phi_b).$$

Metropolis Algorithm

Changes a single site randomly

$$P(\phi_a \to \phi_b) = \begin{cases} e^{S[\phi_a]-S[\phi_b]} & S[\phi_b] > S[\phi_a] \\ 1 & \text{otherwise} \end{cases}$$

Performing this process on every site forms a "sweep"

Wolff Cluster Algorithm

Grows one cluster probabilistically, flips sign[2]

(a) before cluster flip

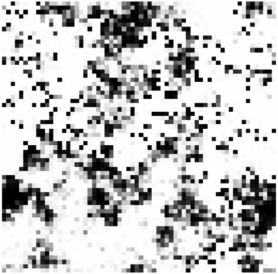

(b) after cluster flip

[2] U. Wolff, Phys. Rev. Lett. **62**, 361 (1989).

Thermalization

How do we start the Markov chain?

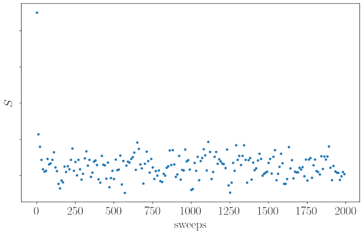

(a) $L = 24$

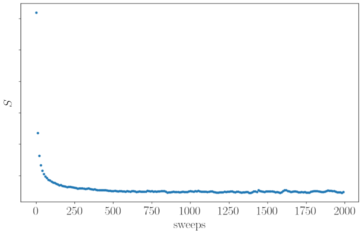

(b) $L = 404$

How do we start the Markov chain?

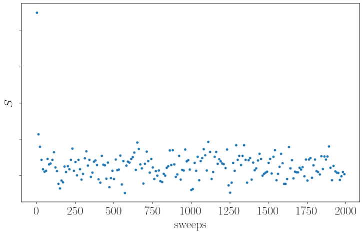

(a) $L = 24$

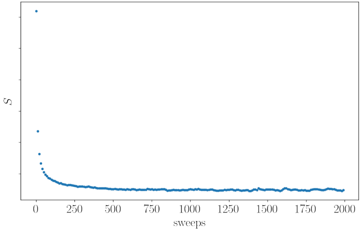

(b) $L = 404$

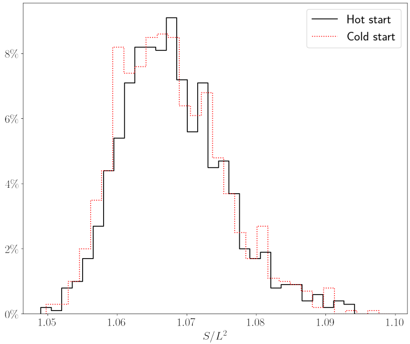

Figure: Action histogram comparing hot vs. cold start after 1000 sweep thermalization

Autocorrelation

How many sweeps per measurement?

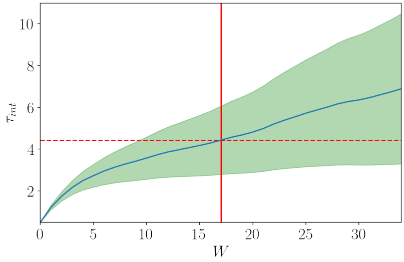

(a) $L = 24$, $\tau_{int} = 4.43$

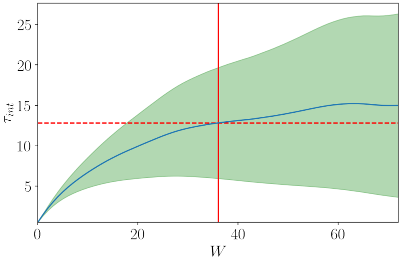

(b) $L = 404$, $\tau_{int} = 12.81$

Figure: Plots of automatic windowing[3] procedure used to calculate τ_{int} for the NLSM model. W is summation window size.

Therefore, we measure every 50 sweeps with a Wolff cluster step every 5 sweeps.

[3] U. Wolff, Computer Physics Communications **176**, 383 (2007).

Topological Charge on the Lattice

Following Berg & Lüsher[4], define topological charge density $q(x^*)$ for each plaquette x^* such that

$$Q = \sum_{x^*} q(x^*)$$

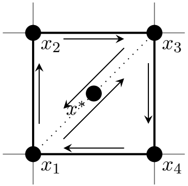

(a) a plaquette

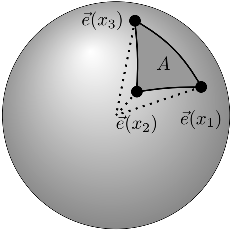

(b) signed area of triangle

$$q(x^*) = \frac{1}{4\pi}\left[A\Big(\vec{e}(x_1), \vec{e}(x_2), \vec{e}(x_3)\Big) + A\Big(\vec{e}(x_1), \vec{e}(x_3), \vec{e}(x_4)\Big)\right].$$

[4] B. Berg and M. Lüscher, Nuclear Physics B **190**, 412 (1981).

Topological Charge Measurement

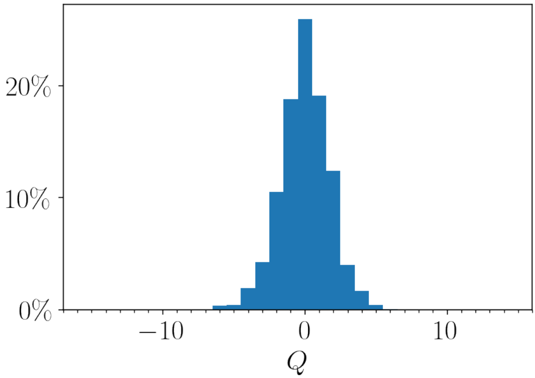

Figure: Histogram of topological charge values Q for trivial NLSM. $L = 404$, 10,000 measurements.

Gradient flow on NLSM

We solve the Gradient Flow numerically using

- fourth-order Runge Kutta
- adaptive step size

ϕ^4 results

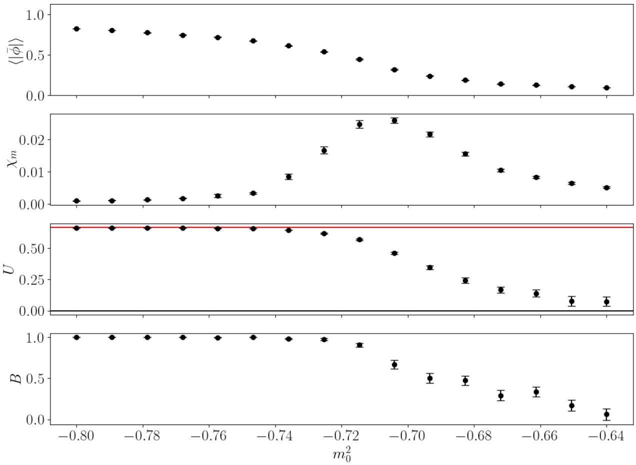

Figure: The lattice average $|\langle\bar{\phi}\rangle|$, the magnetic susceptibility χ_m, the Binder cumulant U [5] and the bimodality B plotted as functions of m_0^2. $L = 64$, $\lambda = 0.5$. 1000 measurements

[5] K. Binder, Zeitschrift für Physik B Condensed Matter **43**, 119 (1981).

Comparison with Berg & Lüscher

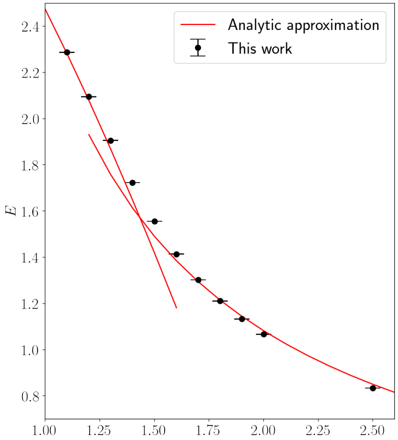

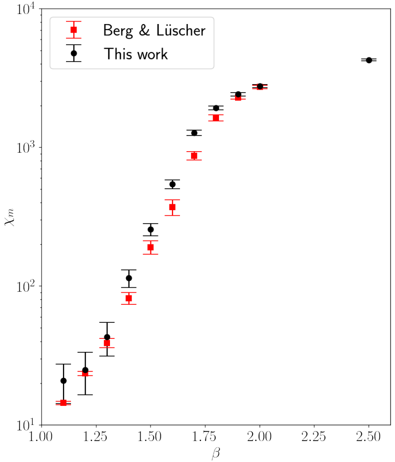

Figure: Comparison with[6], $L = 100$, 1000 measurements.

[6] B. Berg and M. Lüscher, Nuclear Physics B **190**, 412 (1981).

Topological Susceptibility in Flow Time

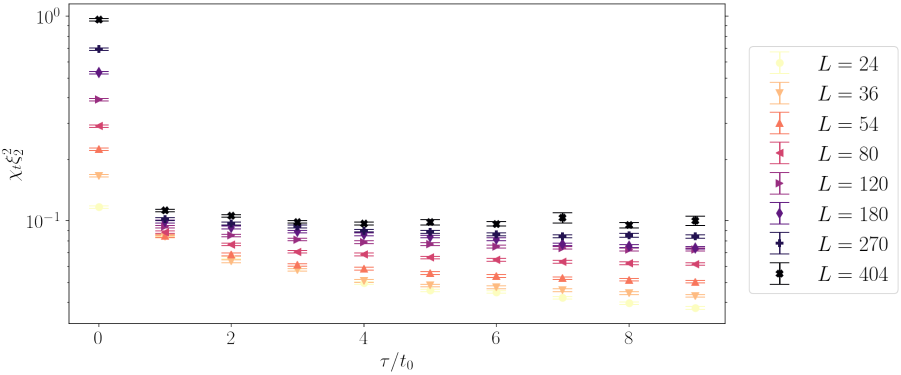

Figure: $\chi_t \xi_2^2$ as a function of flow time τ. Simulation run with 10,000 measurements

χ_t Divergence

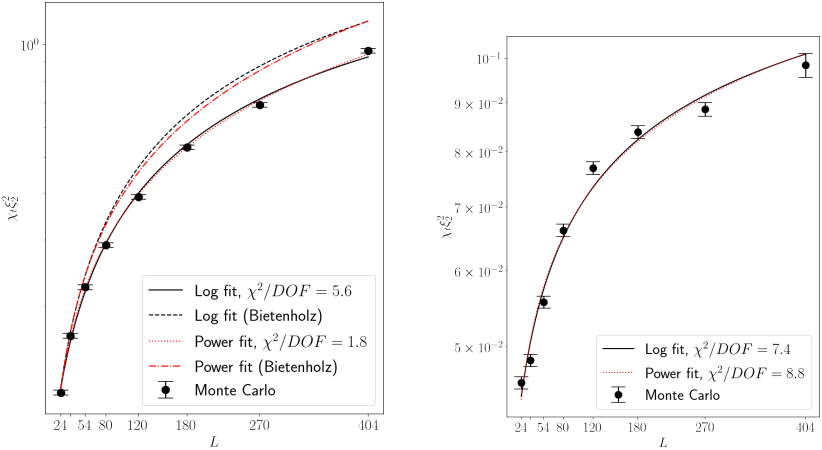

(a) $\tau = 0$ **(b)** $\tau = 5t_0$

Figure: Divergent properties with comparison to[7], 10,000 measurements

[7] W. Bietenholz et al., Phys. Rev. D **98**, 114501 (2018).

Effect of θ-term on $\langle Q \rangle$

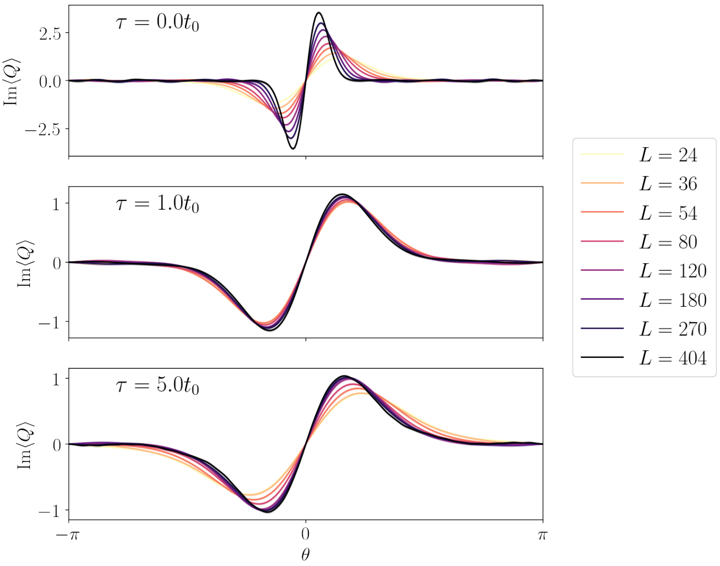

Conclusions

- Berg & Lüscher[8] provide three possible reasons
  1. high-frequency modes cause divergence
  2. the definition of Q is problematic
  3. the NLSM has no well-defined continuum limit

[8] B. Berg and M. Lüscher, Nuclear Physics B **190**, 412 (1981).
[9] M. Bögli et al., J. High Energ. Phys. **2012**, 117 (2012).

Conclusions

- Berg & Lüscher[8] provide three possible reasons
  1. high-frequency modes cause divergence
  2. the definition of Q is problematic
  3. the NLSM has no well-defined continuum limit

[8] B. Berg and M. Lüscher, Nuclear Physics B **190**, 412 (1981).
[9] M. Bögli et al., J. High Energ. Phys. **2012**, 117 (2012).

Conclusions

- Berg & Lüscher[8] provide three possible reasons
  1. high-frequency modes cause divergence
  2. the definition of Q is problematic
  3. the NLSM has no well-defined continuum limit
- Relatively high χ^2/DOF values indicate errors underestimated.

[8] B. Berg and M. Lüscher, Nuclear Physics B **190**, 412 (1981).
[9] M. Bögli et al., J. High Energ. Phys. **2012**, 117 (2012).

Conclusions

- Berg & Lüscher[8] provide three possible reasons
    1. high-frequency modes cause divergence
    2. the definition of Q is problematic
    3. the NLSM has no well-defined continuum limit
- Relatively high χ^2/DOF values indicate errors underestimated.
- Clearer perspective on the effect θ helpful for condensed matter systems[9].

[8] B. Berg and M. Lüscher, Nuclear Physics B **190**, 412 (1981).
[9] M. Bögli et al., J. High Energ. Phys. **2012**, 117 (2012).

Acknowledgements

- 1693 Scholars program (funding for summer research)

Acknowledgements

- 1693 Scholars program (funding for summer research)
- HPC Computing Group

Acknowledgements

- 1693 Scholars program (funding for summer research)
- HPC Computing Group
- Prof. Christopher Monahan

Acknowledgements

- 1693 Scholars program (funding for summer research)
- HPC Computing Group
- Prof. Christopher Monahan
- Friends and family